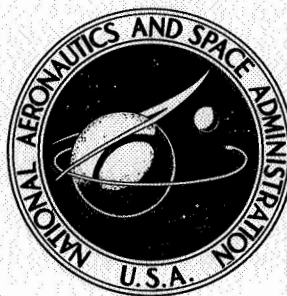


NASA TECHNICAL NOTE



NASA TN D-5008

NASA TN D-5008

HIGH-TEMPERATURE MECHANICAL PROPERTIES
OF POLYCRYSTALLINE HAFNIUM CARBIDE
AND HAFNIUM CARBIDE CONTAINING
13-VOLUME-PERCENT HAFNIUM DIBORIDE

by William A. Sanders and Hubert B. Probst

*Lewis Research Center
Cleveland, Ohio*

NATIONAL AERONAUTICS AND SPACE ADMINISTRATION • WASHINGTON, D. C. • JANUARY 1969

HIGH-TEMPERATURE MECHANICAL PROPERTIES OF POLYCRYSTALLINE
HAFNIUM CARBIDE AND HAFNIUM CARBIDE CONTAINING
13-VOLUME-PERCENT HAFNIUM DIBORIDE

By William A. Sanders and Hubert B. Probst

Lewis Research Center
Cleveland, Ohio

NATIONAL AERONAUTICS AND SPACE ADMINISTRATION

For sale by the Clearinghouse for Federal Scientific and Technical Information
Springfield, Virginia 22151 - CFSTI price \$3.00

ABSTRACT

Hot-pressed, single-phase HfC and HfC containing 13-vol % HfB₂ were tested in three-point transverse rupture to temperatures as high as 4755° F (2625° C). Hot hardness tests were also run to 3200° F (1760° C). Separate effects on the transverse rupture behavior of HfC due to the HfB₂ second phase and due to a grain-size difference are discussed on the basis of strength, deformation, and metallographic results. The probable mechanisms responsible for deformation are also discussed. In hot-hardness tests of HfC containing 13 vol % HfB₂ second phase, a change in the temperature dependency of hot hardness at 2600° F (1425° C) is discussed and related to the degree of cracking around indentations.

HIGH-TEMPERATURE MECHANICAL PROPERTIES OF POLYCRYSTALLINE HAFNIUM CARBIDE AND HAFNIUM CARBIDE CONTAINING

13-VOLUME-PERCENT HAFNIUM DIBORIDE

by William A. Sanders and Hubert B. Probst

Lewis Research Center

SUMMARY

Transverse rupture tests were conducted on single-phase hafnium carbide and hafnium carbide containing 13- volume- percent hafnium diboride as a distinct second phase. These tests were performed between room temperature and 4755°F (2625°C). The test materials were hot pressed to densities in the 95 to 97 percent of theoretical density range.

For the single-phase material at temperatures below about 4000°F (2205°C), strength decreases with increasing temperature, fractures are completely brittle, and the fracture path is transgranular. Above 4000°F (2205°C), strength increases with temperature, some plasticity is present, and fractures are intergranular. Single-phase material of two different grain sizes (8 and $24\text{ }\mu\text{m}$) both exhibited these general features; however, the smaller grain material was stronger at all temperatures.

Below 4000°F (2205°C), the material containing hafnium diboride as second phase exhibited the same general behavior as did the single-phase material, that is, decreasing strength with increasing temperature, brittle behavior, and transgranular fractures. This two-phase material with a grain size of 25 micrometers was, however, stronger than the 24-micrometer grain size single-phase material, which indicates a strengthening brought about by the hafnium diboride. Above 4000°F (2205°C) the two-phase material exhibited plastic behavior and intergranular fractures, similar to single-phase hafnium carbide, however, strength decreases rapidly above 4000°F (2205°C) in sharp contrast to single-phase hafnium carbide.

Metallographic evidence suggests that the plasticity observed in both materials is the result of grain-boundary sliding. In the single-phase material this sliding apparently acts as a stress relieving mechanism preventing premature failures, and, thus, strength increases after 4000°F (2205°C) is reached at which grain-boundary sliding becomes operable. On the other hand, in the two-phase materials, it appears that the portion of the hafnium diboride present in the grain boundaries renders grain-boundary sliding ineffective as a strengthening mechanism, and leads to a rapid loss of strength at temperatures where grain-boundary sliding occurs.

INTRODUCTION

The carbides of the Group IV A transition metals titanium, zirconium, and hafnium, and the Group V A transition metals vanadium, niobium, and tantalum are often suggested for load-bearing members for high-temperature applications. Such suggestions are usually based on the well-known properties of carbides: high melting point and high room-temperature hardness indicative of high stability and high strength.

The chief deterrent to the use of the carbides is their brittleness at temperatures below about one-half their absolute melting points. Without some plastic deformation, stress concentrations at flaws are not relieved, and premature fracture results. However, at higher temperatures, the deformation and strength characteristics of the polycrystalline carbides are not well defined and some beneficial plasticity may be present. Therefore, for a proper assessment of the high-temperature suitability of the carbides, the temperature dependencies for plasticity and strength must be determined. The mechanism by which any plasticity occurs must also be identified.

In the past few years several studies have been reported on the mechanical properties of polycrystalline carbides at high temperatures (refs. 1 to 9). Tantalum carbide (TaC) has been reported to exhibit some ductility starting in the 3185° to 3450° F (1750° to 1900° C) range (refs. 1 to 3). For example, Steinitz (ref. 1) reported tensile strengths and elongations of 15 800 psi (109 MN/m²) and 2 percent and 12 900 psi (89 MN/m²) and 39 percent at 3145° and 3995° F (1800° and 2200° C), respectively. These strengths and elongations reflect the considerable plasticity possible in TaC in combination with high-strength and strength-retention capability. Kelly and Rowcliffe (ref. 3), measured ductile-brittle transition temperatures in bending for the polycrystalline carbides tantalum carbide (TaC), niobium carbide (NbC), vanadium carbide (VC), and titanium carbide (TiC). They found that the ductile-brittle transition occurred at approximately one-half the absolute melting point (homologous temperature, $T_H = 0.5$) for each carbide. These investigators reported a high yield strength of over 59 000 psi (407.1 MN/m²) for titanium carbide at its ductile-brittle bend transition temperature of 2780° F (1525° C) at $T_H = 0.59$. This transition temperature is comparable to the 2915° F (1600° C) temperature ($T_H = 0.61$) at which Keihm and Kebler observed large tensile creep extensions for large grained TiC (ref. 4). Liepold and Nielsen (ref. 5), conducted tensile and tensile creep tests on polycrystalline zirconium carbide (ZrC). At 4350° F (2400° C), a tensile strength for ZrC as high as 11 000 psi (75.9 MN/m²) was measured, and the results of creep tests indicated a change in the creep process at 3905° F (2150° C) for $T_H = 0.65$.

The purpose of this investigation was to determine the high-temperature mechanical behavior of hafnium carbide (HfC; melting point, 7102° F (3928° C)) and, in particular, to find the temperature at which plasticity becomes evident and the mechanism of this

plasticity. To this end, transverse rupture testing was conducted from room temperature to 4755° F (2625° C), and hardness measurements were made from room temperature to 3200° F (1760° C).

Three different varieties (density and grain size combinations) of HfC were studied. All were hot pressed and had densities in the 95 to 97 percent theoretical density range. Extremes of grain sizes were 8 and 25 micrometers. One variety of HfC contained about 13-volume-percent hafnium diboride (HfB₂) as a distinct second phase, while the remaining materials were single phase. The effects of grain size and the second phase on high-temperature mechanical properties were also noted.

MATERIALS AND SPECIMEN PREPARATION

Two lots of HfC powder were used to fabricate bars from which transverse rupture test specimens were made. The chemical and X-ray analyses of the HfC powder lots are given in table I. The major difference between the two powders is the 13-volume-percent

TABLE I. - CHEMICAL AND X-RAY ANALYSES OF HAFNIUM CARBIDE POWDERS

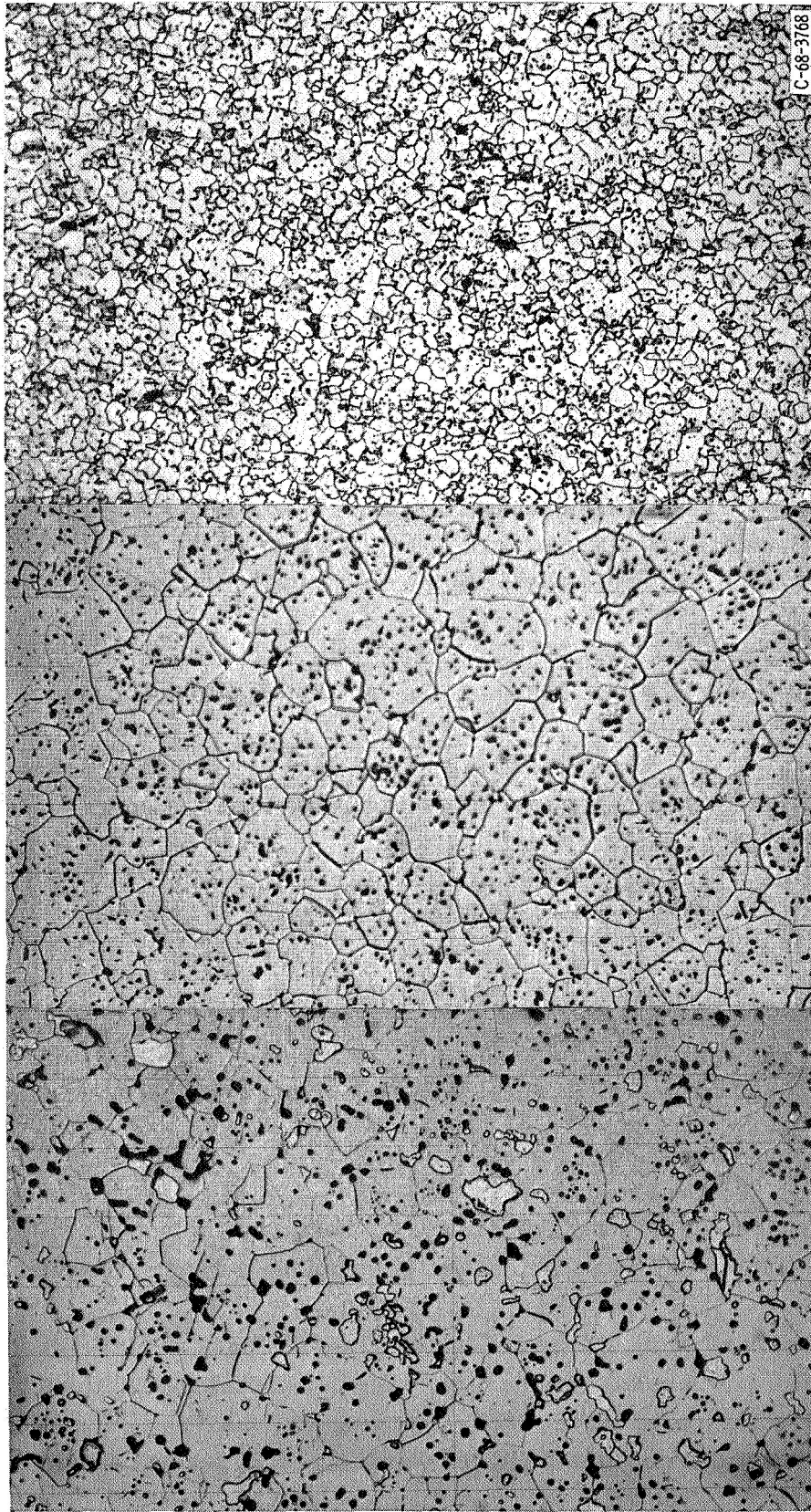
HfC powder lot	Chemical analysis, wt %							X-ray analysis	
	Combined carbon	Free carbon	Boron	Zirconium	Titanium	Oxygen	Nitrogen	Lattice parameter, A (or 10 ⁻¹⁰ m)	Second phase
A	5.92	0.03	0.71	3.40	0.39	^a ND	^a ND	4.631	^b 13 vol % HfB ₂
B	6.29	.04	.005	1.07	.63	0.16	0.03	4.623	None

^aNot determined.

^bBased on X-ray diffraction line intensity ratio versus volume percent HfB₂ calibration determined from standards.

HfB₂ second phase present in the lot A HfC powder. There were also some differences between the two HfC powder lots as to the content of combined carbon, zirconium, and titanium.

Three varieties of bars, 4 by 1/2 by 1/4 inch (102 by 12.7 by 6.3 mm), were made by hot pressing the HfC powders in graphite dies. The hot-pressing conditions for lot A HfC powder were temperature, 4600° F (2535° C); pressure, 2500 psi (17.2 MN/m²); and time, 15 minutes. These conditions yielded compacts of 97 percent density and 25-micrometer grain size. The lot B HfC was commercially hot pressed. Lot B HfC



(a) Lot A: grain size, 25 micrometers; density, 97 percent; white second phase content, 13-volume-percent hafnium diboride. Some porosity due to second phase pull-out.

(b) Lot B: grain size, 24 micrometers; density, 96 percent.

(c) Lot B: grain size, 8 micrometers; density, 95 percent.

Figure 1. - Microstructures of hot-pressed hafnium carbide and hafnium carbide containing 13-volume-percent hafnium diboride. Etchant, 30-volume-percent nitric acid, 10-volume-percent hydrofluoric acid, 60-volume-percent water.

bars were of two varieties: 96 percent density, 24 micrometer grain size and 95 percent density, 8 micrometer grain size. Microstructures of each of the three varieties of bars are shown in figure 1. The HfB_2 second phase in the hot-pressed lot A HfC appears as light equiaxed particles at the grain boundaries and within grains. The pore size and distribution in the three varieties of HfC bars can be said to be similar when allowance is made for pull-out of the HfB_2 second phase during polishing of the lot A HfC.

Transverse rupture test bars, 2 by 0.18 by 0.12 inch (51 by 4.6 by 3.0 mm), and hot-hardness specimens, 0.5 by 0.5 by 0.25 inch (12.7 by 12.7 by 6.4 mm), were cut from the large hot-pressed HfC bars by electric discharge machining. Test pieces were ground lengthwise to final size with a 220-grit diamond wheel. All long edges of the test bars were given a 45° bevel, 0.010-inch (0.25-mm) deep to minimize any edge damage as recommended in American Society for Testing Materials specification B406-64 (ref. 10).

Test bars made from lot A HfC powder which contained the HfB_2 second phase were tested with the tension faces in either the ground or metallographically polished condition. All lot A bars had one side metallographically polished. Most of the bars made from lot B single-phase HfC powder were tested in the ground condition, but a few were tested with metallographically polished tension faces. All hot-hardness specimens were metallographically polished on one 0.5- by 0.5-inch (12.7- by 12.7-mm) face for indentation.

APPARATUS AND EXPERIMENTAL PROCEDURE

Transverse Rupture Testing

Three-point transverse rupture tests in which the support span was 1.5 inches (38.1 mm) were conducted with the apparatus shown schematically in figure 2.

The induction furnace and test fixtures were made from either carbon or high-strength graphite. The induction coil which was powered by a 9600-hertz, 50-kilowatt motor-generator was insulated with stabilized zirconia. Powdered lampblack was used for insulation between the graphite susceptor and the induction coil, and graphite granules were used for insulation above the susceptor lid. A carbon tube topped by a water-cooled right-angle prism provided a sight path for test-bar surface temperature measurement and a means for maintaining an argon atmosphere in the chamber around the HfC test bars. Temperature was measured with an optical pyrometer - prism combination that had been calibrated against a National Bureau of Standards certified standard lamp. A blackbody cavity in a bar heated in the test furnace could not be distinguished from the adjacent surface of the bar; therefore, no correction for emissivity was made. The authors believe that the temperature readings are accurate to $\pm 40^\circ \text{F}$ ($\pm 25^\circ \text{C}$).

On the left of figure 2 is shown the transverse rupture test load train section above the carbon ram. A water-cooled radiation shield connected the carbon ram with a 0-

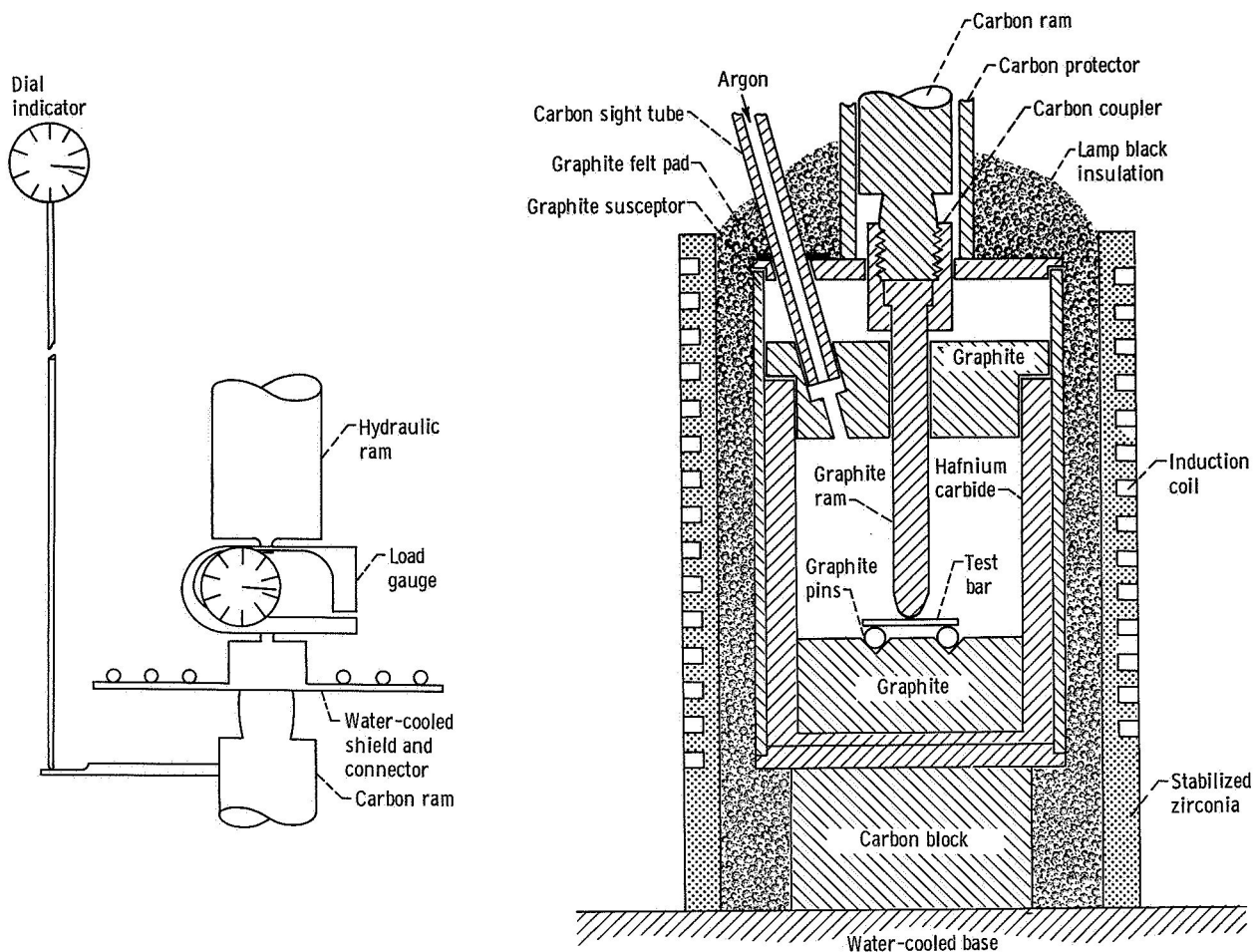


Figure 2. - Transverse rupture test furnace, fixtures, and load train.

to 100-pound compression mechanical force gage. The force gage scale is divided into 1-pound increments, and load could be estimated to the nearest 1/4 pound. The force gage, in turn, was connected to a hydraulic ram actuated by an electric-motor driven pump acting through a pressure regulator. The pressure regulator was operated by a variable-speed motor which permitted maintenance of a constant stress rate. A dial indicator with scale divisions of 0.001 inch was used to measure test-bar deflections. The dial indicator in a fixed position was connected by a vertical-contact pointer to a horizontal metal arm extending from the carbon ram.

Transverse rupture tests were made over the range from room temperature to 4755° F (2625° C). Test bars were heated in a high-purity argon atmosphere at about 100° F per minute (55° C/min) to test temperature and then held at temperature for 10 minutes prior to testing. All tests were conducted at a constant outer-fiber stress rate of 6000 psi per minute (41.4 (MN/m²)/min), and load-deflection readings were taken from the start of loading until fracture. After each test, the fractured bar halves

were fitted together and center-point deformation was measured. Test bars that had metallographically polished faces were examined after test for deformation markings and fracture characteristics.

For all transverse rupture tests, including those in which some small amounts of permanent center-point deformation were measured, the transverse rupture strength σ_T was determined from the formula relating bending moment to elastic stress, such that,

$$\sigma_T = \frac{3Pl}{2bd^2}$$

where

- P center-point load at fracture, lb, N
- l distance between support points, 1.50 in. (38.1 mm)
- b test bar width, 0.180 in. (4.6 mm)
- d test bar depth, 0.120 in. (3.0 mm)

Hot Hardness Testing

A commercial model vacuum hot-hardness-testing furnace was used for the hardness determinations. The furnace temperature controller maintained the desired set temperature to an accuracy of $\pm 20^\circ \text{F}$ ($\pm 13^\circ \text{C}$). The test specimen was supported on a molybdenum platform, and was radiatively heated by a cylindrical molybdenum heating element. A vacuum of about 5×10^{-5} torr could be held at 3200°F (1760°C) with an oil diffusion pump backed by a mechanical pump. The dead-weight loading mechanism of the hardness tester is contained within the vacuum system, and was motorized to permit a controlled lowering rate of a weighted indenter onto the specimen. The indenter material used was 99-percent-dense polycrystalline boron carbide, ground to the Vickers configuration (136° square based pyramid) and mounted in molybdenum holders. A commercial microhardness tester using a Vickers diamond indenter was used for room-temperature hardness measurements.

Hardness tests were made only on the HfC which contained the 13-volume-percent HfB_2 second phase. Tests were conducted at 400°F (222°C) intervals from room temperature to 3200°F (1760°C). A fresh specimen was used for each temperature. A test piece was heated in vacuum at about 100°F per minute (55°C/min) to test temperature, and then held at temperature for 10 minutes prior to indentation. Four indentations per specimen were made using the Vickers polycrystalline boron carbide indenter under a 2500-gram dead-weight load. The loaded indenter was lowered at the rate of 10 millimeters per minute. The indentation diagonals were measured at room temper-

ature using the optical system of the microhardness tester with which the room-temperature hardness measurements were made.

RESULTS AND DISCUSSION

Transverse Rupture Tests

No differences in mechanical behavior were noted between bars tested with tension faces in the ground condition and bars tested with tension faces in the metallographically polished condition.

Deformation. - Permanent center-point deformations at various temperatures are plotted in figure 3, and some deformed bars that are fitted together are shown in figure 4. The highest temperature for which no permanent center-point deformation could be measured for each of the three varieties of HfC bars are represented by the points that fall on the X-axis of figure 3. The lowest temperature at which measureable deformation was observed was 4020°F (2215°C) where a bar containing the HfB_2 second

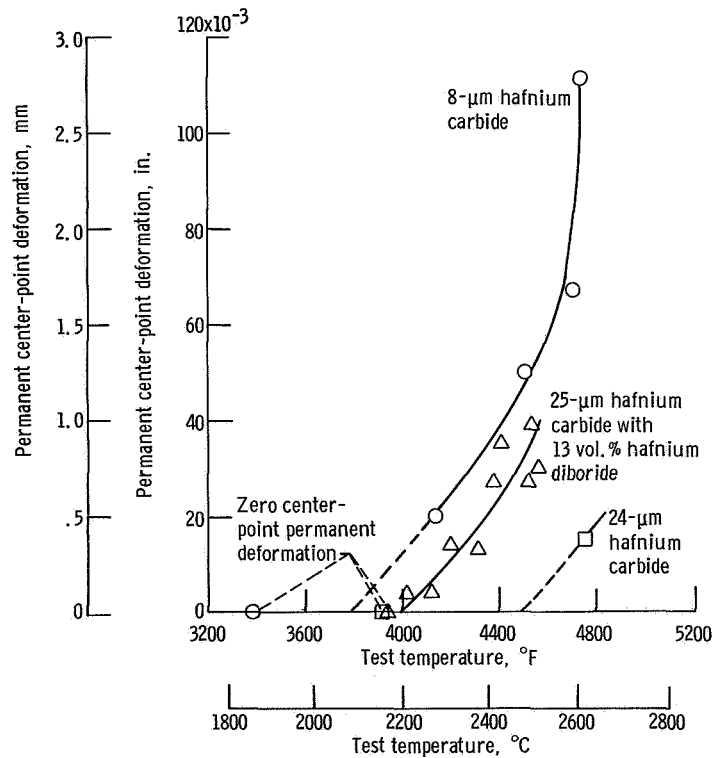
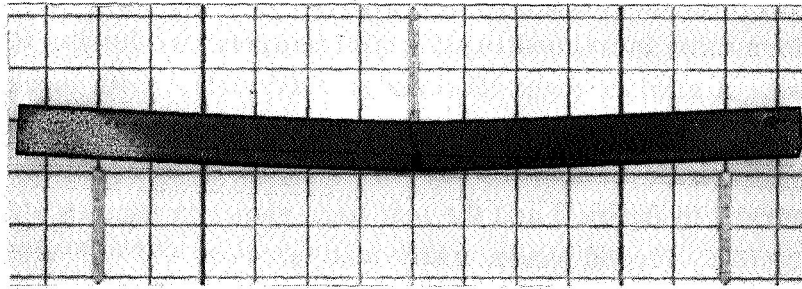
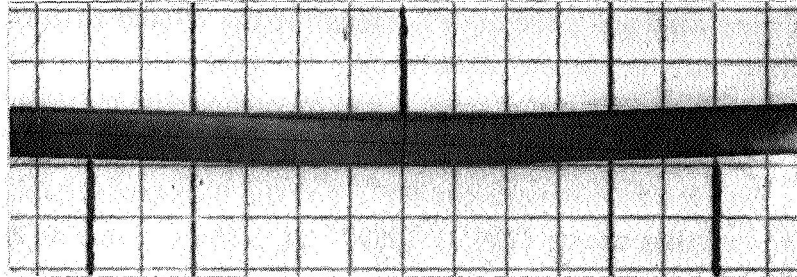


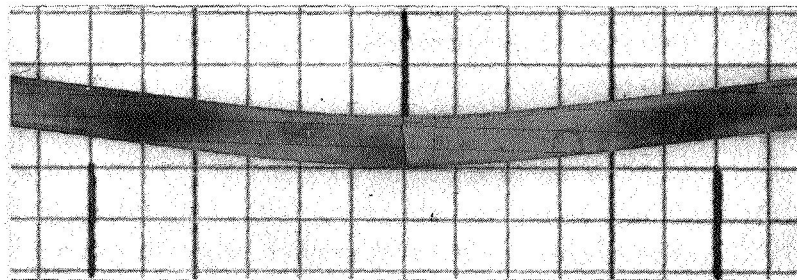
Figure 3. - Effect of temperature on permanent center-point deformation of hafnium carbide and hafnium carbide containing 13-volume-percent hafnium diboride.



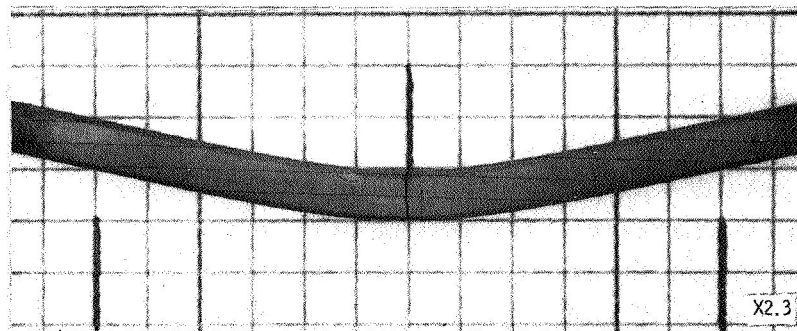
(a) Grain size, 25 micrometers; material, hafnium carbide with 13-volume-percent hafnium diboride; test temperature, 4525° F (2495° C); permanent center-point deformation, 0.027 inch (0.67 mm).



(b) Grain size, 24 micrometers; material, hafnium carbide; test temperature, 4755° F (2625° C); permanent center-point deformation, 0.015 inch (0.37 mm).



(c) Grain size, 8 micrometers; material, hafnium carbide; test temperature, 4715° F (2600° C); permanent center-point deformation, 0.067 inch (1.67 mm).



C-68-3769

(d) Grain size, 8 micrometers; material hafnium carbide; test temperature, 4750° F (2620° C); permanent center-point deformation, 0.111 inch (2.77 mm).

Figure 4. - Permanent center-point deformation of bars of hafnium carbide and hafnium carbide with 13-volume-percent hafnium diboride.

phase showed 0.004-inch (0.10-mm) center-point deformation. Above 4020° F (2215° C), the amount of deformation increased rapidly with temperature for the HfC containing the HfB₂ second phase. A similar rapid increase in deformation with increase in temperature above 4140° F (2280° C) occurred for the 8-micrometer single-phase HfC. An effect of HfB₂ second phase on deformation can be noted by comparing the 24- and 25-micrometer curves in figure 3 and the test bars shown in figures 4(a) and (b). The HfC bar containing HfB₂ second phase, which was tested at 4525° F (2495° C), showed more permanent center-point deformation (0.027 in. (0.67 mm)) than single-phase HfC (0.015 in. (0.37 mm)) which was tested 230° F (130° C) higher at 4755° F (2625° C). Hafnium diboride at the grain boundaries apparently acted to increase deformation.

Although the pore size and pore distributions for the 8- and 24-micrometer single-phase HfC materials may be somewhat different, an apparent grain size effect on deformation in the single-phase HfC can also be noted by comparing the 8- and 24-micrometer curves in figure 3 and the test bars in figures 4(b) to (d). The 8-micrometer HfC is much more deformable than the 24-micrometer HfC, and the 8-micrometer material is rapidly increasing in deformability above 4715° F (2600° C). The greater deformability for the finer grain material suggests an important role played by the grain boundaries in the deformation of the HfC.

Modulus of rupture. - Modulus of rupture data for the three varieties of HfC are plotted in figure 5 as a function of temperature. With increase in temperature the strength of the 24-micrometer single-phase HfC and the 25-micrometer HfC containing HfB₂ second phase at first decreased at similar rates. The HfC with HfB₂ second phase was consistently stronger to about 3500° F (1930° C). Since low-temperature brittle fractures ordinarily originate at a grain boundary (ref. 11), the greater strength of the HfC containing HfB₂ second phase might be attributed to grain-boundary strengthening due to that portion of the HfB₂ present at grain boundaries.

Above about 3500° F (1930° C), the 24-micrometer single-phase HfC and the 25-micrometer HfC containing HfB₂ second phase displayed different strength-temperature behaviors. For 25-micrometer HfC with HfB₂ second phase, the strength-temperature behavior became erratic, and, at about 4000° F (2205° C), the strength began to decrease rapidly. At the highest test temperature (4620° F (2545° C)), the strength had dropped to 5000 psi (34.5 MN/m²). The erratic strength behavior beginning at about 3500° F (1930° C) is attributed to that portion of the second-phase HfB₂ at grain boundaries. In contrast, the strength of single-phase, 24-micrometer HfC was beginning to increase by 4000° F (2205° C) ($T_H = 0.59$) and was still apparently increasing in strength to 27 100 psi (187 MN/m²) at the highest test temperature (4755° F (2625° C)). At the highest temperature at which HfC with HfB₂ second phase was tested, 4620° F (2545° C), the single-phase HfC was about five times stronger.

The 8-micrometer, single-phase HfC was the strongest material tested as shown

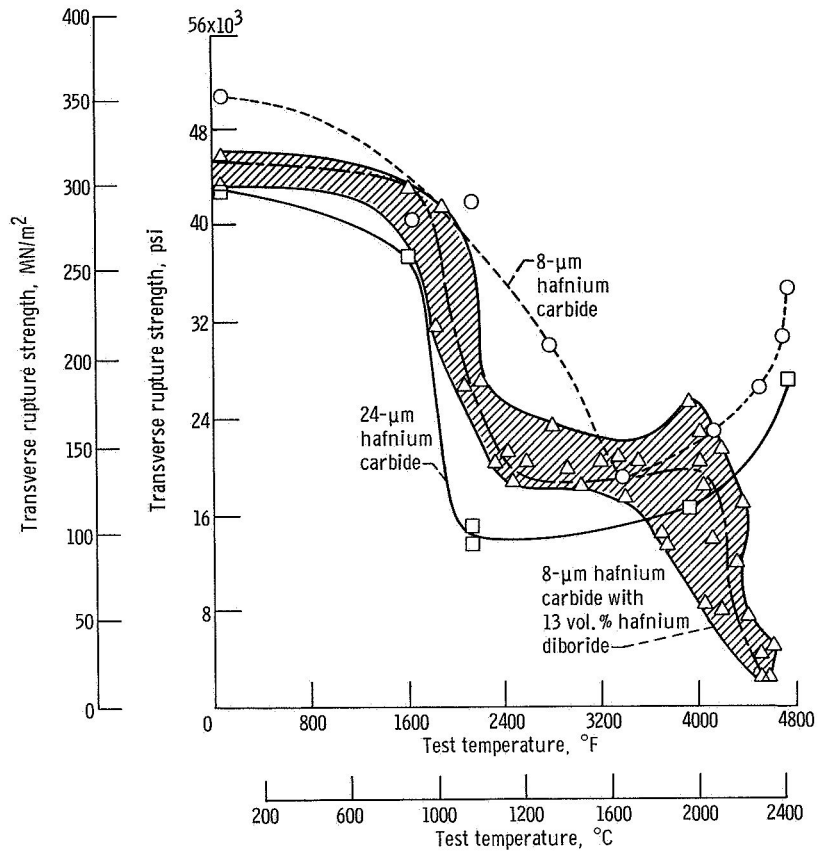


Figure 5. - Effect of temperature on transverse rupture strength of hafnium carbide and hafnium carbide with 13-volume-percent hafnium diboride.

in figure 5. The strength did not drop as rapidly above 1600° F (870° C) as did the 24-micrometer HfC. Rather, the strength of the 8-micrometer HfC decreased gradually from room temperature to 3400° F (1870° C). The higher strength for the finer grain material is consistent with the usual effect of grain size on rupture strength of brittle materials (ref. 12). Certainly by 4000° F (2205° C) ($T_H = 0.59$), the strength of 8-micrometer HfC was increasing with increasing temperature. This strength-temperature behavior was about the same as that for the 24-micrometer single-phase HfC, but the 8-micrometer material was stronger. At the highest test temperature (4750° F (2620° C)), the strength of 8-micrometer HfC was 34 900 psi (241.5 MN/m²). The authors believe that these increases in strength with increasing temperature for both 8- and 24-micrometer single-phase HfC are due to relaxation of stress concentrations afforded by grain-boundary sliding. Grain-boundary sliding would inhibit the propagation of a crack nucleated within a grain and would also retard the nucleation of cracks at any flaws in the grain boundaries. Both effects are stress-relieving actions that would be beneficial by allowing the attainment of higher applied stresses before

fracture. In the next section some metallographic evidence for grain-boundary sliding will be presented.

To compare the strength-temperature behavior observed for the 8-micrometer single-phase HfC with other carbides, some recently reported modulus of rupture data and the data of this investigation are plotted in figure 6. At room temperature, the strength of HfC compares well with the high strength of niobium carbide (NbC) and is much higher than the strength of TaC. The great strength increase for TiC reported by Kelly and Rowcliffe (ref. 3), starting near the ductile-brittle transition temperature 2780°F (1527°C) ($T_H = 0.59$), is similar to the behavior observed for HfC. The beginning of the strength increase for HfC also occurred at $T_H = 0.59$ but the increase

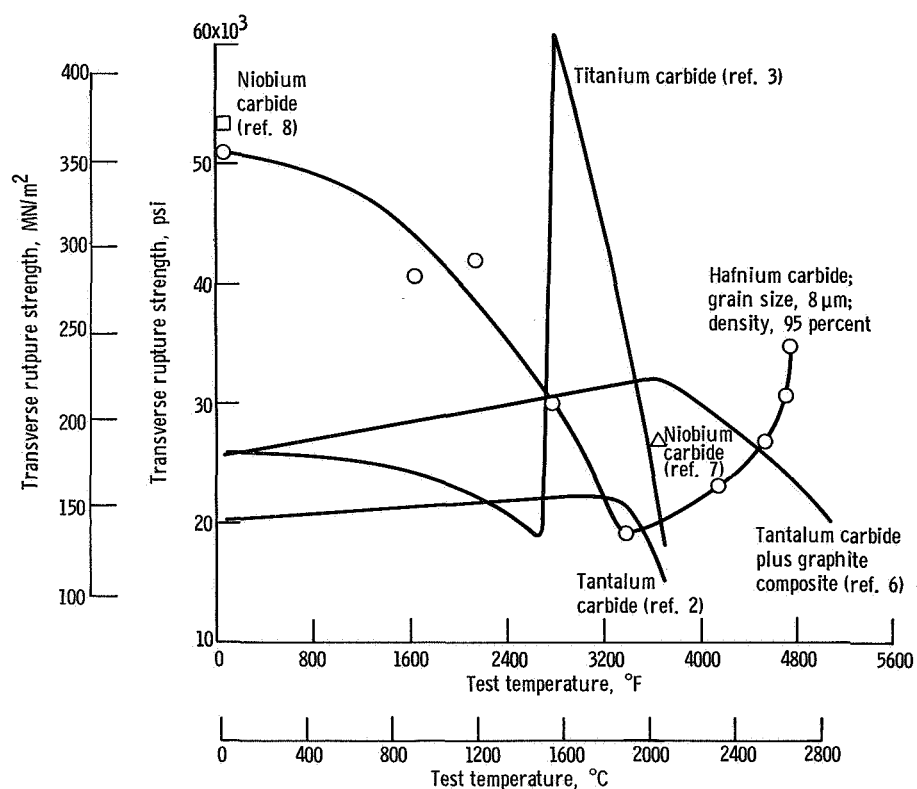


Figure 6. - Effect of temperature on transverse rupture strength of carbides.

was less abrupt and sustained over a much greater temperature range. Kelly and Rowcliffe (ref. 3) have attributed the increase in strength of TiC at $T_H = 0.59$ to local plastic flow which may relieve stresses at internal or surface flaws. The strength drop

observed for TiC^1 was attributed to general plastic yielding.

Above 3700° F (2035° C) HfC is the only carbide increasing in strength. And above 4500° F (2480° C) HfC is stronger than the strongest known tantalum carbide plus carbon ($\text{TaC} + \text{C}$) composite (ref. 6).

Microstructures

The microstructures presented and discussed in this section are for HfC with HfB_2 second phase. However, the observations made apply also to all the single-phase HfC test bars examined after test.

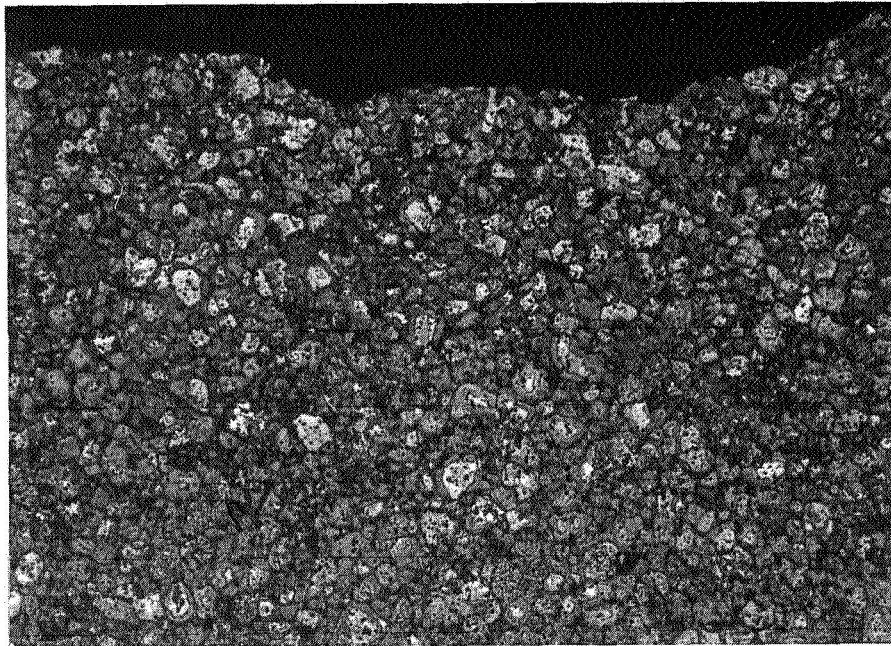
The lowest temperature indication of the predominating influence of grain boundaries on fracture is an observed change in fracture characteristic occurring between 3930° and 4200° F (2165° and 2315° C). In figure 7 the tension faces at fracture of bars tested at 3930° F (2165° C) and 4200° F (2315° C) show a change from transgranular to intergranular fracture. The lowest temperature at which center-point deformation of a test bar occurred was 4020° F (2215° C), which is in the temperature region where the fracture mode changed.

Other metallographic features observed in this study are illustrated in figure 8. These photomicrographs were taken after fracture; however, the surfaces shown were metallographically polished prior to transverse rupture testing. In both figures the HfB_2 second phase is indistinguishable from the HfC matrix due to tarnishing of the pre-polished bar surface which occurred during the test conducted in the flowing argon atmosphere. When tested bars are lightly repolished, the second-phase HfB_2 is once more apparent. The interpretation of features illustrated in figure 8 is the result of examining many samples, not just the two shown in these figures.

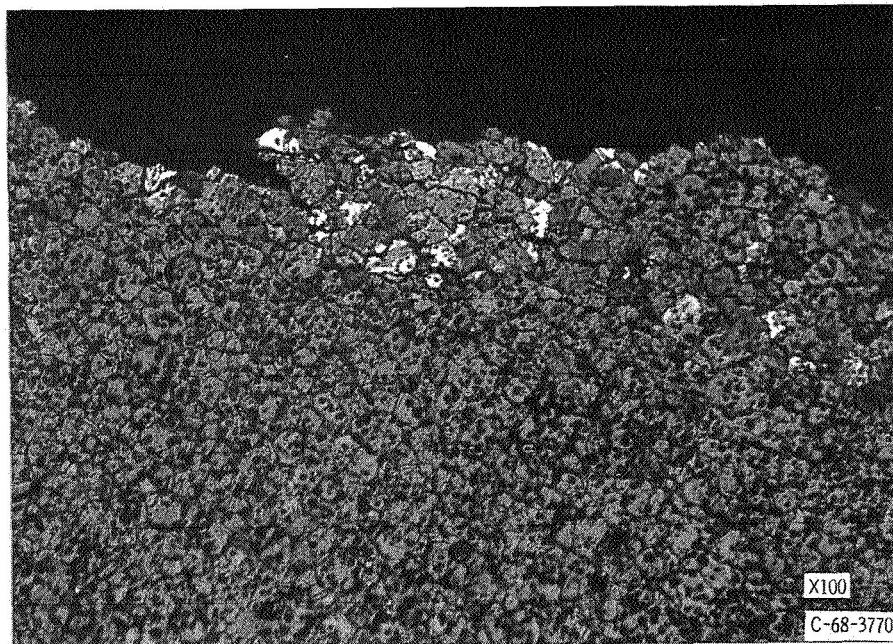
The faint double boundaries in figure 8(a) appear to be the result of grain-boundary migration. This is boundary motion in a direction generally perpendicular to its surface as occurs in grain growth. However, the migration observed here does not appear to be solely a thermal effect. Such doubling of boundaries was observed throughout the stressed portion of bars but not near the ends (unstressed regions). Thus, the observed grain-boundary migration appears to be stress induced.

The very dark and wide-grain boundaries in figure 8 are interpreted as the result of grain-boundary sliding, that is, the displacement or shearing of a grain with respect to an adjacent grain in a direction generally parallel to the surface of the grain boundary.

¹The strength values from Kelly and Rowcliffe at temperatures above 2800° F (1540° C) are actually yield strengths and not fracture strengths. Their test apparatus did not allow straining to fracture above 2800° F (1540° C .) However, they reported very little strain hardening for TiC above 2800° F (1540° C); therefore, the values plotted in figure 6 are believed to be close to the fracture strengths.

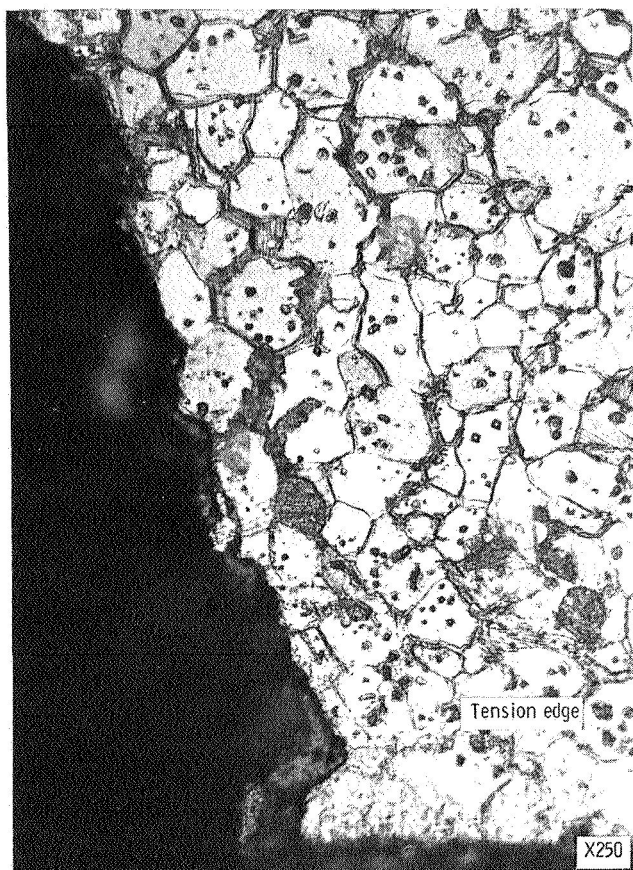


Transgranular fracture at 3930° F (2165° C).

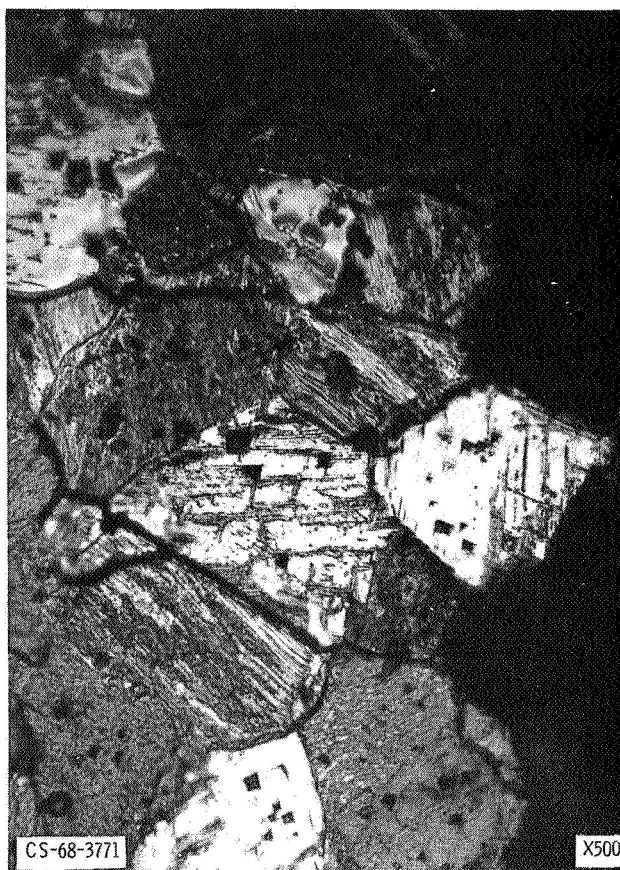


Intergranular fracture at 4200° F (2315° C).

Figure 7. - Fracture characteristics for hafnium carbide containing 13-volume-percent hafnium diboride; tension face at fracture.



(a) Bar side at fracture; test temperature, 4310° F (2375° C).



(b) Bar tension face at fracture; test temperature, 4525° F (2495° C).

Figure 8. - Metallographic indications of grain-boundary migration, grain-boundary sliding, and crystallographic slip in hafnium carbide containing 13-volume-percent hafnium diboride.

More detailed features of grain-boundary sliding are shown in figure 8(b). These are the casting of a shadow of one grain onto an adjacent grain indicating relative displacement between the two grains, and the rumpling of grain surfaces near grain boundaries.

Parallel markings within grains, indicative of crystallographic slip, are most apparent in figure 8(b). Such markings were only observed in a few grains near the fracture surface. This observation, in addition to the fact that the gross shape of grains was unchanged after testing, suggests that slip is a minor deformation mode. It appears that crystallographic slip contributes to the gross permanent deflection only inasmuch as it contributes to grain boundary sliding; that is, the rumpling of grain surfaces to allow boundary sliding must occur by slip.

Based on the metallographic evidence, it appears that the plasticity exhibited by HfC at temperatures above 4000° F (2205° C) is predominantly the result of grain-boundary sliding with crystallographic slip playing only a minor role. From the evidence at hand, this conclusion would appear to apply to both single-phase HfC and the material containing 13-volume-percent HfB₂.

Hot-Hardness Tests

The results of the hot-hardness test made only on the 25-micrometer HfC containing HfB₂ second phase are shown on a semilogarithmic plot in figure 9. Also plotted are some hardnesses of NbC and TiC recently reported by Koester and Moak (ref. 13) and the hardnesses of some arc-melted and centrifugally cast (AMCC) single-phase HfC recently reported by Adams, et al., (ref. 14). The NbC was tested over the temperature range 1830° to 3270° F (1000° to 1800° C), or 0.33 to 0.53 T_H, and the TiC was tested over the temperature range 1830° to 2915° F (1000° to 1600° C) or 0.38 to 0.56 T_H. The AMCC HfC was tested from room temperature to 2735° F (1500° C), or 0.42 T_H. On such a semilogarithmic plot as is shown in figure 9, a change in slope has been attributed to a change in the plastic flow mechanism for metals (refs. 15 and 16) and aluminide intermetallic compounds (ref. 17). An inflection in the plot for the HfC containing the HfB₂ second phase did occur at about 2600° F (1425° C), or T_H = 0.40, but the NbC and TiC materials showed no inflection and were softer in the 1800° to 3200° F (980° to 1760° C) measurement range. The AMCC HfC also did not show an inflection, although it was tested to a temperature 135° F (75° C) above the inflection temperature observed for the HfC containing the HfB₂ second phase. Also, the AMCC

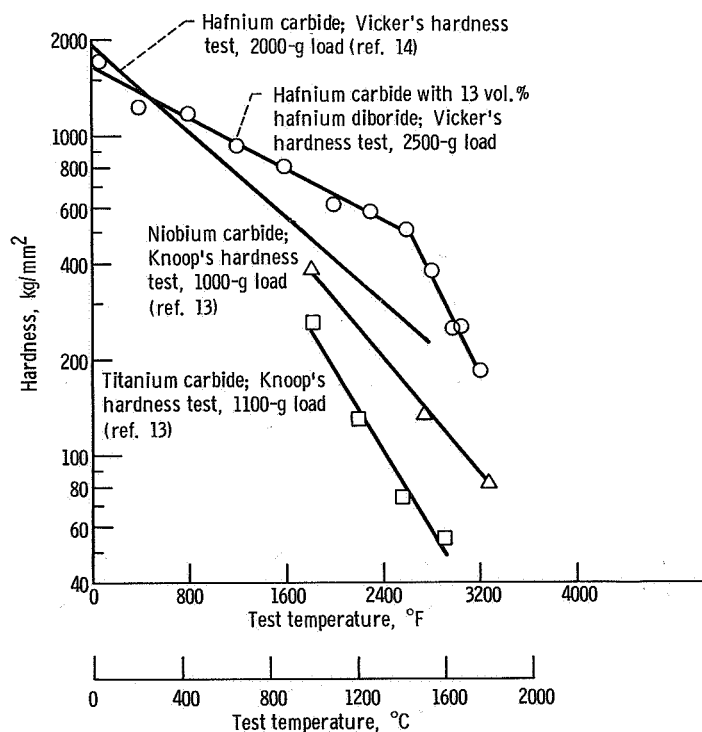
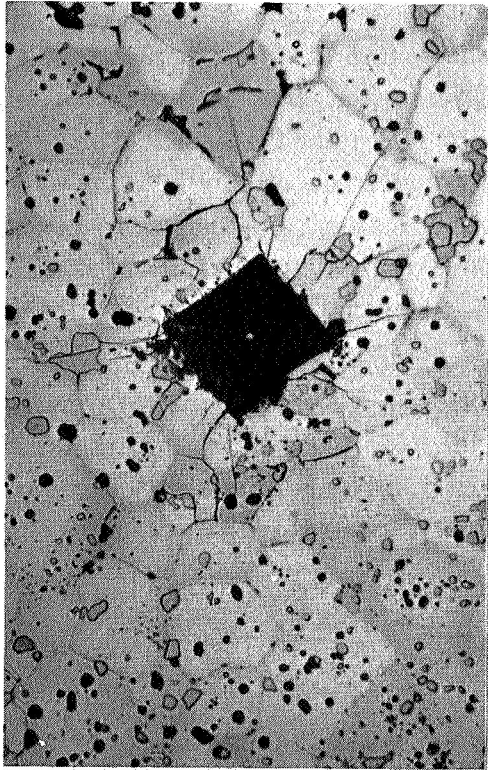
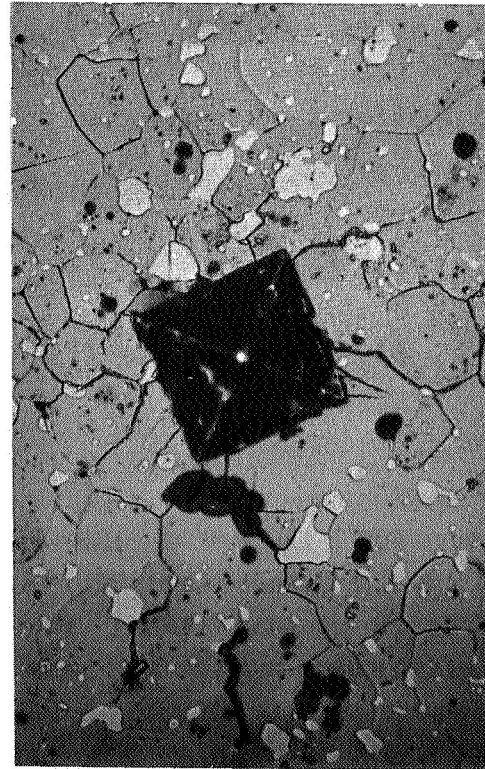


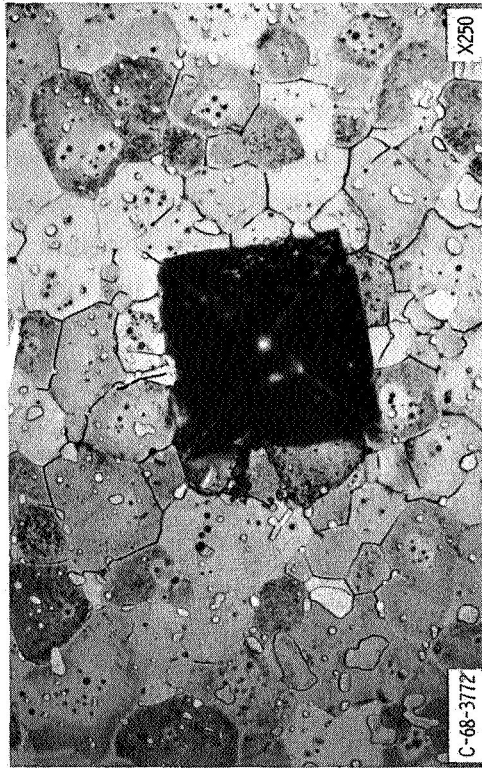
Figure 9. - Effect of temperature on hardness of hafnium carbide containing 13-volume-percent hafnium diboride and other carbides.



Temperature, 1600° F (870° C).



Temperature, 2600° F (1425° C).



Temperature, 2975° F (1635° C).

Figure 10. - Hot hardness indentations in hafnium carbide containing 13-volume-percent hafnium diboride.

HfC was generally softer than the HfC containing the HfB_2 second phase. This hardness difference may be due to the difference in combined carbon content: 5.5 weight percent for the AMCC HfC against 5.9 weight percent for the HfC containing HfB_2 . Adams, et al., (ref. 14) have observed that the higher the combined carbon content for single-phase AMCC HfC, the higher the hot hardness to 2735°F (1500°C).

The change in the slope of the semilogarithmic hardness plot for the HfC containing HfB_2 second phase (fig. 9) coincided with a cessation of cracking around the indentations. Figure 10 shows indentations made in vacuum at 1600°F (870°C), 2600°F (1425°C), $T_H = 0.40$, the inflection temperature, and 2975°F (1635°C). The 1600°F (870°C) indentation is accompanied by many cracks, but the 2600°F (1425°C) indentation has only a few cracks. The 2975°F (1635°C) indentation is essentially crack-free. Petty (ref. 17) has attributed inflection temperatures and cessation of cracking in aluminide intermetallic compounds to a change in the deformation mode. But, in this case, for the HfC containing HfB_2 second phase, it is difficult to reconcile the apparent plastic-deformation mechanism that prevents cracking at a temperature of only 2600°F (1425°C) or $T_H = 0.40$ with the fact that measureable plasticity was not observed in transverse rupture tests until a temperature of 4020°F (2215°C), or $T_H = 0.59$ was reached. It should be noted that the stress states involved in hardness testing and transverse rupture testing are, of course, different. Possibly, the stress state produced by the hardness test (essentially a creep condition in which no predetermined strain rate is imposed) allows some dislocation motion and, thus, prevents crack nucleation. On the other hand, the rather high strain rate imposed in transverse rupture testing would not favor dislocation motion until a higher temperature is reached.

CONCLUDING REMARKS

This study has resulted in a description of the mechanical behavior of hot-pressed HfC from room temperature to nearly 4800°F (2650°C). For single-phase HfC, as temperatures increase, bend strength decreased, followed by increased strength near the high end of the temperature range. Below about 4000°F (2205°C), this material behaved in a completely elastic manner, gave brittle fractures, and the fracture path was transgranular. Above 4000°F (2205°C), HfC exhibited some degree of plasticity, and the fracture path was intergranular. Metallographic evidence indicated that this plasticity is the result of grain-boundary sliding. When grain-boundary sliding is operable, strength increases with increasing temperature. This is believed to be due to the stress relieving action brought about by grain-boundary sliding. By grain-boundary sliding, stress concentrations can be relieved preventing premature failure and thus allowing higher applied stresses to be reached before fracture.

At all test temperatures, the finer grain HfC ($8\text{ }\mu\text{m}$ as opposed to $24\text{ }\mu\text{m}$) gave superior strengths.

The material containing 13-volume-percent HfB_2 as a second phase showed the same general behavior as the single-phase material up to about 4000°F (2205°C). In this temperature range, the two-phase material was totally elastic, brittle, and fractured transgranularly. However, when compared with single-phase material, there was some strengthening noted in the two-phase material. This strengthening can be attributed to the HfB_2 second phase; however, the exact mechanism by which this second phase strengthens in the elastic region is not clear.

As with the single-phase material, above 4000°F (2205°C), the HfB_2 -containing material exhibits some plasticity and an intergranular fracture path. This plasticity also appears to be the result of grain-boundary sliding; however, grain-boundary sliding in the two-phase material is accompanied by a drastic loss of strength. Apparently, when grain-boundary sliding starts at about 4000°F (2205°C), which is a high homologous temperature of 0.68 for HfB_2 , that portion of the HfB_2 located at the grain boundaries is too weak to sustain sliding as a stress relieving mechanism but, rather, allows complete fracture through the grain boundaries.

Lewis Research Center,
National Aeronautics and Space Administration,
Cleveland, Ohio, October 22, 1968,
129-03-04-07-22.

REFERENCES

1. Steinitz, Robert: Mechanical Properties of Refractory Carbides at High Temperatures. Nuclear Applications of Non-Fissionable Ceramics. Alvin Boltax and J. H. Handwerk, eds., Am. Nucl. Soc., 1966, pp. 75-100.
2. Johansen, H. A.; and Cleary, J. G.: The Ductile-Brittle Transition in Tantalum Carbide. J. Electrochem. Soc., vol. 113, no. 4, Apr. 1966, pp. 378-381.
3. Kelly, A.; and Rowcliffe, D. J.: Deformation of Polycrystalline Transition Metal Carbides. J. Am. Ceramic Soc., vol. 50, no. 5, May, 1967, pp. 253-256.
4. Keihn, F.; and Kebler, R.: High-Temperature Ductility of Large-Grained TiC. J. Less-Common Metals, vol. 6, 1964, pp. 484-485.
5. Leipold, Martin H.; and Nielsen, Thomas H.: Mechanical Properties of Hot-Pressed Zirconium Carbide Tested to 2600°C . J. Am. Ceramic Soc., vol. 47, no. 9, Sept. 1964, pp. 419-424.

6. Harada, Y.: Metal Carbide-Graphite Composites. Quarterly Rep. no. 1, IIT Research Inst. (NASA CR-79757), Oct. 27, 1966.
7. Harada, Y.: Metal Carbide-Graphite Composites. Rep. IITRI-G6005-06, IIT Research Inst. (NASA CR-92723), Jan. 25, 1968.
8. Merryman R. G.; Robertson, R. H.; and Dietz, R. J.: The Room Temperature Flexural Strength of Some Metal Carbide-Carbon Composites Hot Pressed by CMB-6. Rep. LASL-N-1-1824, Los Alamos Scientific Lab., Oct. 25, 1966.
9. Leipold, M. H.; and Nielsen, T. H.; The Mechanical Behavior of Tantalum Carbide and Magnesium Oxide. Rep. JPL-TR-32-1201, Jet Propulsion Lab., California Inst. Tech. (NASA CR-90511), Dec. 1, 1967.
10. Anon.: Determination of Transverse Rupture Strength of Cemented Carbides. ASTM Designation B406-64, ASTM Standards, Part 7, Mar. 1966.
11. Stokes, R. J.: The Role of Defects on the Mechanical Properties of Nonfissionable Ceramics. Nuclear Applications of Non-Fissionable Ceramics. Alvin Boltax and J. H. Handwerk, eds., Am. Nucl. Soc., 1966, pp. 3-29.
12. Spriggs, R. M.; Vasilos, T.; and Brissette, L. A.: Grain Size Effects in Polycrystalline Ceramics. Materials Science Research, Vol. 3. Plenum Press, 1966, p. 313.
13. Koester, R. D.; and Moak, D. P.: Hot Hardness of Selected Borides, Oxides, and Carbides to 1900^o C. J. Am. Ceramic Soc., vol. 50, no. 6, June 1967, pp. 290-296.
14. Adams, Robert P.; Copeland, M. I.; Deardorff, D. K.; and Lincoln, R. L.: Cast Hafnium Carbide-Carbon Alloys: Preparation, Evaluation, and Properties. Rep. BM-RI-7137, Bureau of Mines, June 1968, p. 36.
15. Westbrook, J. H.: Temperature Dependence of the Hardness of Pure Metals. Trans. ASM, vol. 45, 1953, pp. 221-248.
16. Petty, E. R.: Hardness and Other Physical Properties of Metals in Relation to Temperature. Metallurgia, vol. 56, no. 337, Nov. 1957, pp. 231-236.
17. Petty, E. R.: Hot Hardness and Other Properties of Some Binary Intermetallic Compounds of Aluminum. J. Inst. Metals, vol. 89, 1960-61, pp. 343-349.

POSTMASTER: If Undeliverable (Section 158
Postal Manual) Do Not Return

"The aeronautical and space activities of the United States shall be conducted so as to contribute . . . to the expansion of human knowledge of phenomena in the atmosphere and space. The Administration shall provide for the widest practicable and appropriate dissemination of information concerning its activities and the results thereof."

—NATIONAL AERONAUTICS AND SPACE ACT OF 1958

NASA SCIENTIFIC AND TECHNICAL PUBLICATIONS

TECHNICAL REPORTS: Scientific and technical information considered important, complete, and a lasting contribution to existing knowledge.

TECHNICAL NOTES: Information less broad in scope but nevertheless of importance as a contribution to existing knowledge.

TECHNICAL MEMORANDUMS: Information receiving limited distribution because of preliminary data, security classification, or other reasons.

CONTRACTOR REPORTS: Scientific and technical information generated under a NASA contract or grant and considered an important contribution to existing knowledge.

TECHNICAL TRANSLATIONS: Information published in a foreign language considered to merit NASA distribution in English.

SPECIAL PUBLICATIONS: Information derived from or of value to NASA activities. Publications include conference proceedings, monographs, data compilations, handbooks, sourcebooks, and special bibliographies.

TECHNOLOGY UTILIZATION PUBLICATIONS: Information on technology used by NASA that may be of particular interest in commercial and other non-aerospace applications. Publications include Tech Briefs, Technology Utilization Reports and Notes, and Technology Surveys.

Details on the availability of these publications may be obtained from:

SCIENTIFIC AND TECHNICAL INFORMATION DIVISION
NATIONAL AERONAUTICS AND SPACE ADMINISTRATION
Washington, D.C. 20546